18th International Conference
ENGINEERING MECHANICS 2012
Svratka, Czech Republic, May 14 – 17, 2012

pp. 269–279
Paper #318

BLAST PERFORMANCE OF FRC COMPOSITES

M. Foglar*, M. Kovář**

Abstract: *The paper presents ways of numerical modeling of RC and FRC slabs subjected to blast loading. The models are based on experiments which were described at the EM2011, the experiments are performed in the military training area Boletice with the cooperation with the Czech Army. The use of racture energy as the key quantity in the modeling of FRC in comparison to RC is studied.*

Keywords: ***blast loading, fiber concrete, reinforced concrete.***

1. Introduction

This paper presents the primary results of two sets of field tests of blast performance of reinforced concrete and reinforced concrete specimens with plastic fibers. The tests were performed in cooperation with the Czech Army corps and Police of the Czech Republic at the military training area Boletice using real scale precast slabs and 25 kg of TNT charges placed in distance from the slab for better simulation of real in-situ conditions.

2. Field tests of blast performance of reinforced concrete and reinforced concrete specimens with plastic fibres

2.1. Specimens

This paper continues the research presented at Engineering Mechanics in 2011 (Foglar & al., 2011).

The specimens are designed in real scale of a small span bridge in as concrete slabs, 6m long, 1,5m wide and 0,3m thick. For reinforcing details, see referenced paper.

Five specimens were used in total during the experiments performed in 2010 and 2011. Three of the specimens were made of C30/37 grade concrete (specimen No. 1 (2010), 2 (2010) and 5 (2011)), two of C55/67 grade concrete (No. 3 (2011) and 4 (2011)). Polypropylene 54mm long synthetic fibres were used in three of the specimens. The fibre dosage was following: specimen No. 1 - 0kg/m3, No. 2 – 4,5kg/m^3, No. 3 - 0 kg/m^3, No. 4 – 4,5 kg/m^3 and No. 5 - 9kg/m^3. The dosage of the fibres was kept low as it can be achieved on-site. The fiber tensile strength is 620-758MPa, the shape combines monofilament and fibrillated shape (slightly corrugated and blended with fibrillated PolyPropylene fibers).

2.2. Results of the experiments

The experiments showed the beneficiary effect of added fibers on blast performance of the specimens.

The specimen No. 1, C30/37, no fibres, is regarded as the reference specimen. This specimen is the most damaged one by the blast loading. The area of the puncture is 0,43m^2, volume 0,12m^3, which represents 4,4% of the total volume of the specimen. Total volume of the damaged concrete (puncture + spalling) is 0,23m^3, which represents 8,5% of the total volume of the specimen. The sides of the specimen were damaged severely. The deflection was 295mm on the left side and 310mm on the right

* Ing. Marek Foglar, Ph.D.: Department of concrete and masonry structures, Czech Technical University, Thákurova 7; 166 29, Prague; CZ, e-mail: marek.foglar@fsv.cvut.cz

** Ing. Martin Kovář: Department of concrete and masonry structures, Czech Technical University, Thákurova 7; 166 29, Prague; CZ, e-mail: martin.kovar@fsv.cvut.cz

side of the specimen. The shape of deflection was similar to deflection from uniformly distributed loading.

The specimen No. 2, C30/37, 4,5kg/m^3 PP fibres was less damaged. The area of the puncture is 0,26m^2, volume 0,08m^3, which represents 2,9% of the total volume of the specimen. Total volume of the damaged concrete (puncture + spalling) is 0,15m^3, which represents 5,6% of the total volume of the specimen. The area of puncture was reduced by 40% in comparison to specimen No. 1, the total volume of damaged concrete was reduced by 35% in comparison to specimen No. 1. The left side of specimen No. 2 was not damaged, the damage of the right side was reduced by more than 50%. The deflection was 365mm on the left side and 380mm on the right side of the specimen. The shape of deflection was similar to deflection from point loading in the mid-span of the specimen. The deflection was increased by 19% in comparison to specimen No. 1.

The specimen No. 5, C30/37, 9kg/m^3 PP fibres was less damaged. Total volume of the damaged concrete (puncture + spalling) is 0,06m^3, which represents 2,2% of the total volume of the specimen. There was no puncture, the total volume of damaged concrete was reduced by 75% in comparison to specimen No. 1. The sides of specimen No. 5 were not damaged. The deflection was 255mm on the left side and 265mm on the right side of the specimen. The shape of deflection was similar to deflection from point loading in the mid-span of the specimen. The deflection was decreased by 16% in comparison to specimen No. 1.

The specimen No. 3, C55/67, no fibres was less damaged. The area of the puncture is 0,02m^2, volume 0,01m^3, which represents 0,4% of the total volume of the specimen. Total volume of the damaged concrete (puncture + spalling) is 0,2m^3, which represents 7,4% of the total volume of the specimen. The area of puncture was reduced by 95% in comparison to specimen No. 1, the crushed concrete remained within the reinforcement matrix, total volume of damaged concrete was reduced by 15% in comparison to specimen No. 1. The damage to the sides was reduced by 85%. The deflection was 285mm on the left side and 290mm on the right side of the specimen. The shape of deflection was similar to deflection from uniformly distributed loading. The deflection was increased by 10% in comparison to specimen No. 1.

The specimen No. 4, C55/67, 4,5kg/m^3 PP fibres was less damaged; its damage was similar to specimen No. 5. Total volume of the damaged concrete (puncture + spalling) is 0,05m^3, which represents 1,9% of the total volume of the specimen. There was no puncture, the total volume of damaged concrete was reduced by 22% in comparison to specimen No. 1. The sides of specimen No. 5 were not damaged. The deflection was 300mm on the left side and 305mm on the right side of the specimen. The shape of deflection was similar to deflection from point loading in the mid-span of the specimen. The deflection was increased by 15% in comparison to specimen No. 1.

The differences in puncture and spalling of concrete on the soffit of the slabs can be found in Table 1. The effect of blast loading on top and bottom surfaces of the specimens can be found in Fig. 1.

Tab. 1: Comparison of blast performance of specimens.

Specimen No.	**1**	**2**	**3**	**4**	**5**
Concrete	C30/37	C30/37	C55/67	C55/67	C30/37
Fibres	-	4,5kg/m^3	-	4,5kg/m^3	9,0kg/m^3
Puncture – top surface	0,43 m^2	0,26 m^2	0,02 m^2	-	-
Concrete spalling (soffit) < concrete cover	2,35 m^2	1,89 m^2	1,51 m^2	0,73 m^2	0,61 m^2
Concrete spalling (soffit) > concrete cover	1,71 m^2	1,09 m^2	1,2 m^2	0,44 m^2	0,37 m^2
Concrete spalling (top surface) < concrete cover	0,43 m^2	0,26 m^2	0,89 m^2	0,68 m^2	0,66 m^2
Concrete spalling (top surface) > concrete cover	0,43 m^2	0,26 m^2	0,29 m^2	0	0,08 m^2
Concrete spalling (left side) < concrete cover	0,52 m^2	0,05 m^2	0,08 m^2	0	0
Concrete spalling (left side) > concrete cover	0,35 m^2	0	0,02 m^2	0	0
Concrete spalling (right side) < concrete cover	0,34 m^2	0,16 m^2	0,08 m^2	0	0
Concrete spalling (right side) > concrete cover	0,23 m^2	0,11 m^2	0,02 m^2	0	0
Volume of crushed concrete	0,23 m^3	0,15 m^3	0,20 m^3	0,05 m^3	0,06 m^3
Permanent deflection	0,31 m	0,37 m	0,28 m	0,30 m	0,26 m

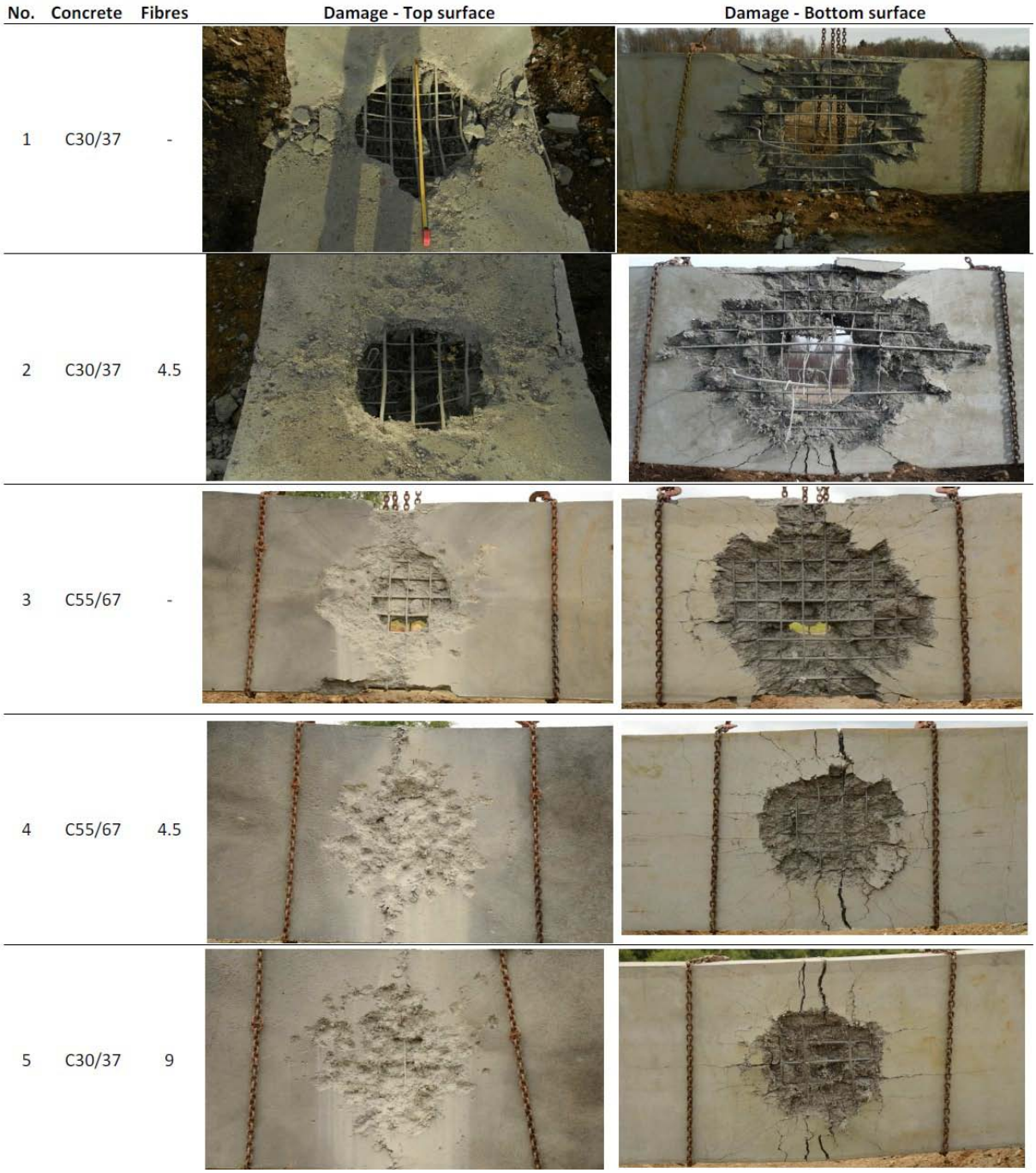

Fig. 1: Top and bottom surface of the RC specimen with plastic fibers after the blast.

3. Numerical modeling

A numerical model of the experiment was prepared for the purpose of further research. The process of model set-up is described in the following text. The model was calibrated according to the outcomes of the experiments described in the previous chapter.

3.1. Numerical solution of fast dynamic phenomena

Fast dynamic phenomena can be solved by the method of explicit time integration (finite difference method, differential method, see Fig, 2) the equation of motion can be expressed as

$$M_n \cdot u_n'' + C_n \cdot u_n' + K_n \cdot u_n = p_n \tag{1}$$

is solved in time t_n, hence at the start of fixed time step.

The method is based on linear displacement change. The velocity

$$u'_{n+1/2} = \frac{1}{\Delta t_{n+1/2}}(u_{n+1} - u_n) \tag{2}$$

is inserted into equation of acceleration

$$u'' = \frac{1}{\Delta t_n}(u'_{n+1/2} - u'_{n-1/2}) \tag{3}$$

u_{n+1} remains unknown in Eq. (1). The displacement in time t_{n+1} is

$$\begin{aligned}&(\frac{1}{\Delta t^2}M_n + \frac{1}{2\Delta t}C_n)\cdot u_{n+1} = \\ &p_n - (K_n - \frac{2}{\Delta t^2}M_n)\cdot u_n - (\frac{1}{\Delta t^2}M_n - \frac{1}{2\Delta t}C_n)\cdot u_{n-1}\end{aligned} \tag{4}$$

The matrixes M and C are diagonal; the solution is fast and simple.

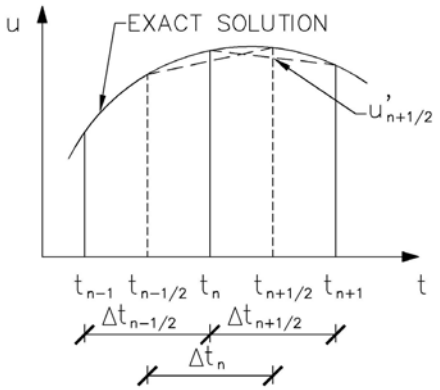

Fig. 2: The explicit time integration method (finite difference method)

In the method of explicit time integration, the system is in equilibrium only at time t_n, but not at time t_{n+1}. The time step depends on the highest natural frequency of the structural system. If the time step is adequately small, the method is numerically stable. The method of explicit time integration solves small number of equations in very small time steps in duration of approximately $10^{-6} – 10^{-8}$ s. The method of explicit time integration is suitable only for processes of a very short duration.

3.2. Numerical modeling of the experiments

LS-DYNA solver was developed for non-linear analysis of fast dynamic phenomena like blast or impact. Within the calculation, the FEM mesh can adapt by deleting elements whose resistance was depleted; these FEM elements “erode”.

The model composes of several parts. The air forms boundaries of the model; the explosive (e.g. TNT) transfers the energy from the blast to FE elements of the air, where the blast wave propagates. The concrete specimen is modeled by solids, reinforcement by beam elements. For example of the model, see Fig. 3.

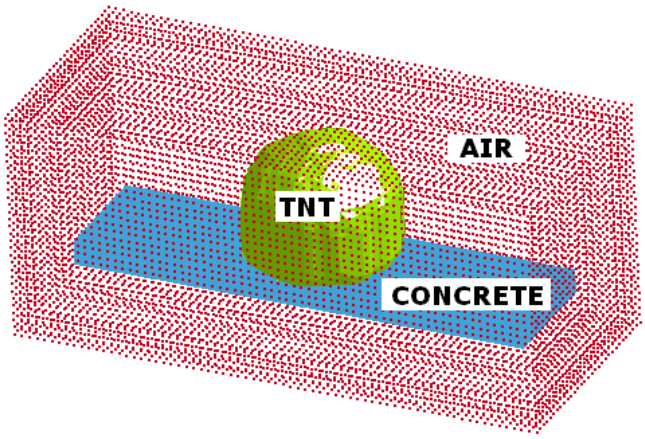

Fig. 3: Set-up of the FE model

The air is modeled using the 009-Null material and forms the undeformable FE network. The concrete specimen is modeled by the 159- CSCM_Concrete material model (brittle material model with damage (Murray (2007)); similar approach to concrete modeling is used by Coughlin et al. (2010)). The explosive is modeled by the 008-High explosive burn material model. The blast overpressure is calculated by the JWL equation of state (EOS):

$$p = A\left(1 - \frac{\omega}{R_1 V}\right)e^{-R_1 V} + B\left(1 - \frac{\omega}{R_2 V}\right)e^{-R_2 V} + \frac{\omega E}{V} \tag{5}$$

The material parameters of the used model (including strain-rate dependent response) were automatically generated in the LS-DYNA from the particular concrete compressive strength. The material properties of the FRC (fracture energy and others) are currently tested, see below.

3.2.1. 2D model

As the first step, a 2Dmodel was prepared. Its goal was to show basic characteristics of the experiment, e.g. the time when the blast overpressure wave reaches the surface of the specimen, the time when the elements at the soffit the specimen start to erode, etc. The blast overpressure wave reaches the surface of the specimen at 0,25 ms, see Fig. 4.

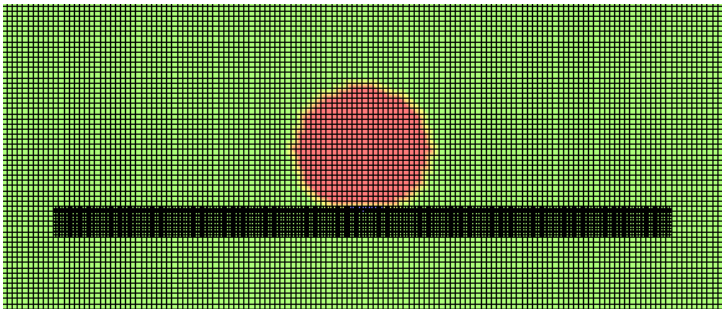

Fig. 4: Blast overpressure wave at 0,25 ms

The first finite elements start to erode at 0,4 ms, see Fig. 5.

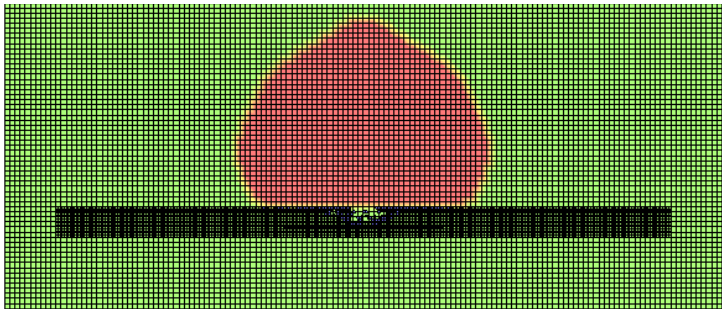

Fig. 5: Blast overpressure wave at 0,5 ms

Fig. 6 compares the video-recorded blast overpressure wave during the experiment with the FE model; element erosion can be spotted under the hypocenter.

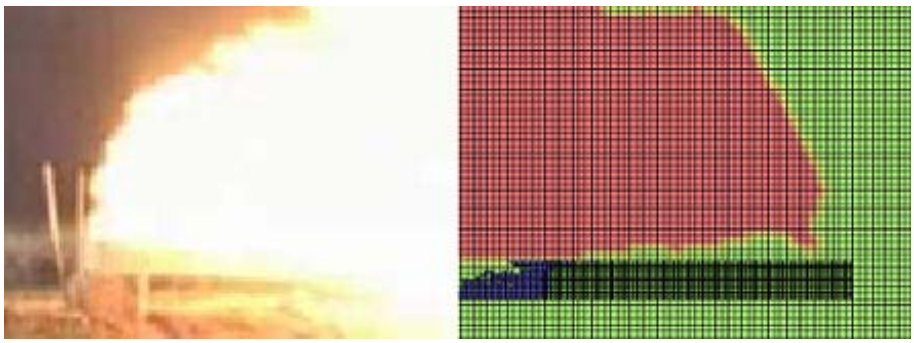

Fig. 6: Experiment vs. FE model

3.2.2. 3D model of reinforced concrete specimens

The 3D reinforced concrete model was prepared to mitigate the weaknesses of the plain concrete model using real dimensions of longitudinal and transverse reinforcement incl. links (steel reinforcement modeled as beam elements). The mesh size was chosen 30mm for concrete and reinforcement and 50mm for air.

The first elements erode when the blast overpressure wave reaches the surface under the hypocenter at 0,25 ms.

In the following phase, more FE erode, the damage of the specimen increases and spalling at the soffit takes place. For results at 1 ms from the blast, top surface and soffit, see Fig. 7, 8. Fig. 7 shows plastic strain (crack development) for plain concrete. Fig. 8 compares two slabs with different concrete grade (C30/37xC55/67 reinforced concrete).

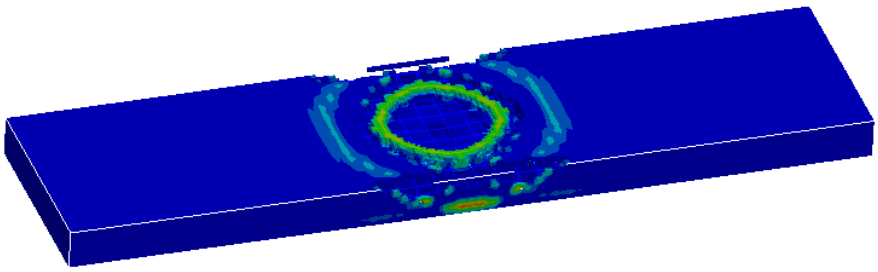

Fig. 7: Top view of the plain concrete specimen after the blast (t = 1 ms)

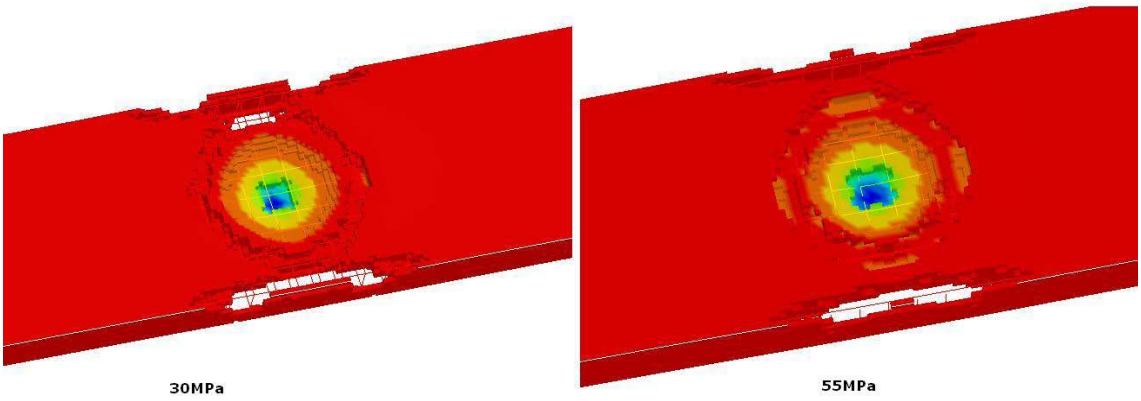

Fig. 8: Damage of two reinforced concrete specimens (left C30/37, right C50/67) (t = 1 ms)

The results of numerical modeling show good agreement with the experiments for reinforced concrete specimens.

3.3. 3D model of reinforced concrete specimens with PP fibers

The behavior of fiber concrete subjected to blast load is quite different from the behavior of plain (respectively reinforced) concrete specimens. At plain concrete, the specimen fails in tension after reaching its tensile strength. At fiber concrete, the stiffness of the specimen decreases after the tensile strength is reached (strain softening). The fibers take over the tensile stress during strain softening and the material performs with a residual tensile strength (approximately 1/3 of the original tensile strength according to fiber type, dosage and geometry). The difference between stress-strain diagrams of plain concrete and fiber concrete can be seen in Fig. 9.

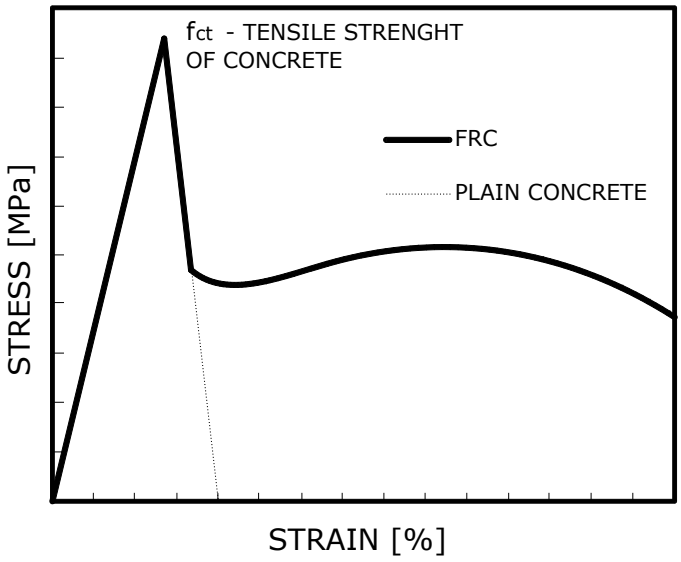

Fig. 9: Stress-strain diagram of concrete material model with damage

The material model of plain concrete MAT159_CSCM (material model with damage and plasticity, Murray, Y.D. (2007)) used in LS-DYNA solver has to be recalibrated to perform according to the presented description, i.e. to provide ductile behavior. For the analytical decription of the MAT159_CSCM material model, see Fig. 10.

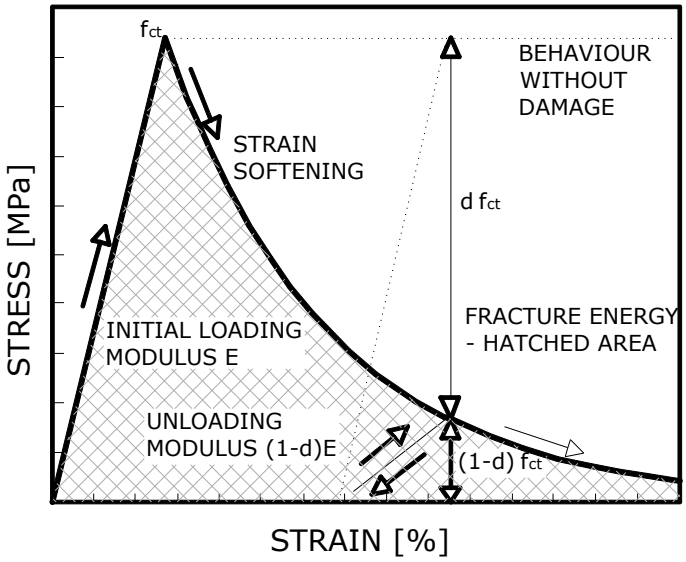

Fig. 10: Stress-strain diagram of concrete material model with damage

The key to MAT159_CSCM material model recalibration lies in tuning its unloading part to describe behavior of fiber concrete while the loading part can remain unchanged (the difference of plain concrete and fiber concrete can be neglected). The fracture energy G_f can be can be expressed as an integral of the area below the stress-strain diagram:

$$G_f = \int_0^{\infty} (1-d) f_{ct} dx \tag{6}$$

Where: d is the damage (from 0 to 1) and f_{ct} is the tensile strenght.

According to this approach, the integral of the fracture energy is used for verification of the value of the fracture energy.

The FRC material model was calibrated according to experiments decribed by Drahorad, Foglar et al. (2011). The experiments studied the strain-rate effect of FRC specimens (700x150x150mm) subjected to 4 points bending (see Fig. 11). The concrete mix properties and fiber dosage were the same as in the field experiments. The finite elements size in the numerical model used for evaluation of the experiments was chosen the same as in the full scale 3D models described in the preceeding paragraphs, as the blast modeling is highly scale-sensitive.

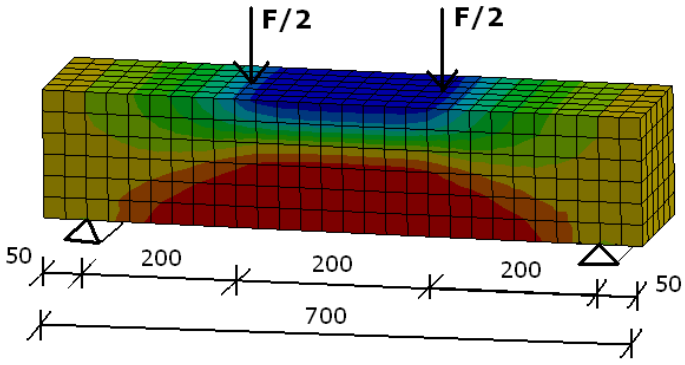

Fig. 11: Layout of the control experiment (mm)

The calibration models were prepared using LS-DYNA for plain concrete and both dosages of PP fibers. The fracture energy in tension and shear of the material model of plain concrete was modified to obtain similar integral of the fracture energy both from the experiments and the numerical evaluation.

For comparison of the force-deflection (F-δ) diagrams of plain concrere, 4,5kg/m^3 and 9kg/m^3 PP fibers FRC both experimental and numerical, see Fig. 13. The area of the force-deflection deigram was limited to the deflection of 8mm.

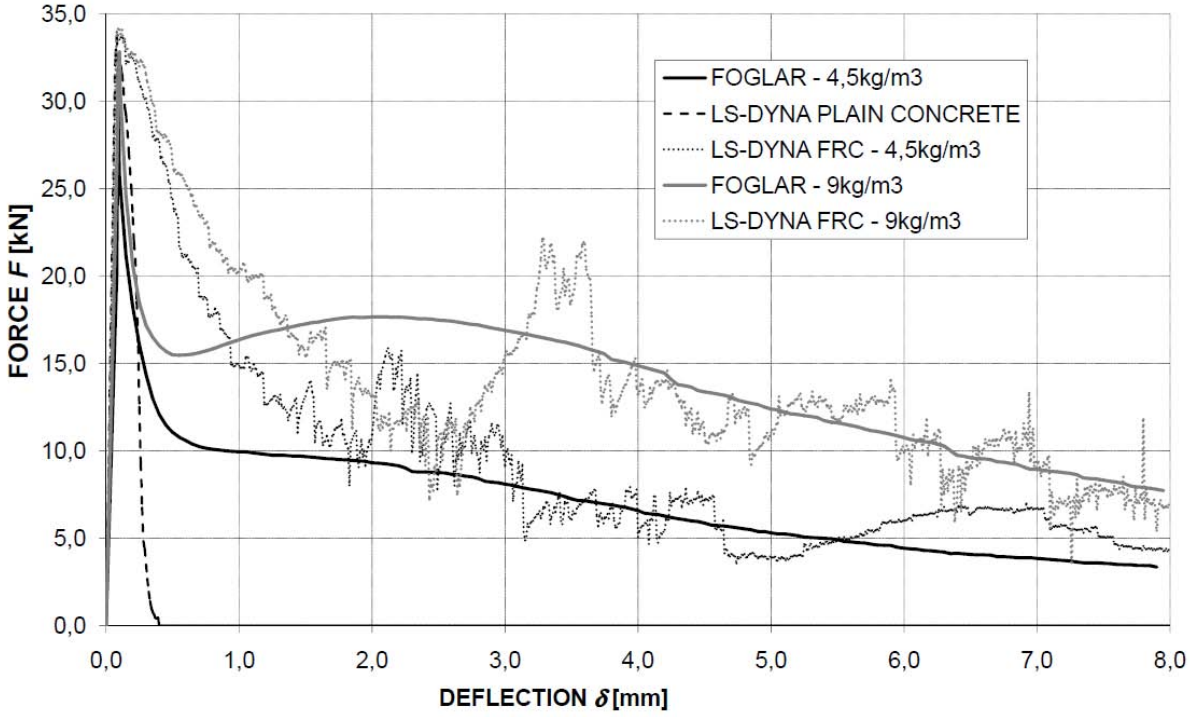

Fig. 13: Force – deflection diagram of material models

The obtained values of the fracture energy for various concrete strength classes and fiber dosages can be seen in Table 2.

Tab. 2: Hodnoty lomových energií různých betonů

Specimen	Fracture energy [N/m]
LS-DYNA – plain concrete	5,6
C30/37 – 4,5 kg/m^3 - experimental	62,0
C30/37 – 4,5 kg/m^3 - numerical	68,6
Foglar C30/37 – 9 kg/m^3	109,3
LS-DYNA – FRC with 9 kg/m^3	102,9

The calibrated material model was used in the 3D models described in the previous chapter. For example of the result of the modeling, see Fig. 14.

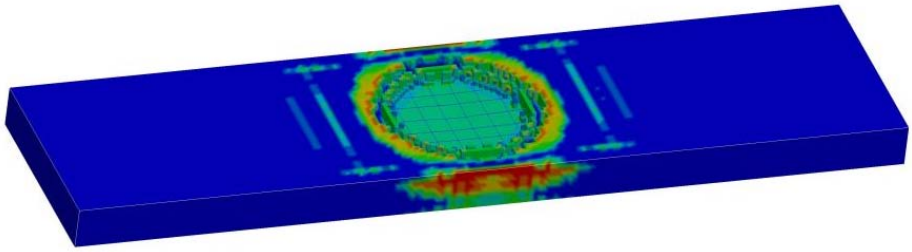

Fig. 14: Top view of the FRC specimen after the blast (t = 1 ms)

The results of numerical modeling show very good agreement with the experiments for specimens with added fibers.

4. Conclusions

The paper continued the paper presented at Engineering Mechanics 2011 with the results for high performance concrete and higher fiber dosages.

The experiments showed beneficiary effect of added fibres on blast performance of the specimens. The experiments also showed beneficiary effect of increased concrete compressive strength on blast performance of the specimens. Combination of fibres and increased compressive strength proved itself to be very effective for improving the blast performance.

The way of modeling of fiber concrete subjected to blast loading by increasing the facture energy of plain concrete MAT159_CSCM material model was presented and evaluated. The model calibration was performed according to small scale experiments. The results of numerical modeling show very good agreement with the experiments for specimens with added fibers.

Other ways of modeling of fiber concrete subjected to blast loading lie in changing the area of plasticity of the material model or in modeling of the dispersed reinforcement. These methods require much more effort to be invested, yet the result remains questionable.

Acknowledgement

This paper was supported by the Czech Ministry of Industry and Trade project FR-TI3/531 and the and the CTU project No. SGS12/029/OHK1/1T/11.

References

Coughlin A.M., Musselman E.S., Schokker A.J., D.G. Linzell (2010), Behavior of portable fiber reinforced concrete vehicle barriers subject to blasts from contact charges, *International Journal of Impact Engineering*, Volume 37, Issue 5, pp. 521-529.

Drahorád M., Foglar M., Smiřinský S., Veselý M. (2012), Užití dynamického faktoru nárůstu pevnosti betonu pro zkrácení doby zkoušek vláknobetonových vzorků, *Beton TKS 1/2012,* pp. 74-79.

Foglar M., Sochorová E., Kohoutková A. (2011), Field tests of blast performance of reinforced concrete and fibre reinforced cocncrete specimen, *Engineering mechanics*, pp. 143-146.

Millard, S.G. & al. (2010) Dynamic enhancement of blast resistant ultra high performance fiber-reinforced concrete under flexural and shear loading. *International Journal of Impact Engineering*, 37, 4, pp. 405-413.

Murray, Y.D. (2007), *User Manual for LS-DYNA Concrete Material Model 159*, US Department of transportation, FHWA-HRT-05-062

Murray, Y.D. (2007), *Evaluation of LS-DYNA Concrete Material Model 159*, US Department of transportation, FHWA-HRT-05-063